The Springtime North Asia Cyclone Activity Index and the Southern Annular Mode

YUE Xu[1,2] (乐 旭) and WANG Huijun*[1] (王会军)

[1] *Nansen-Zhu International Research Centre (NZC), Institute of Atmospheric Physics (IAP), Chinese Academy of Sciences (CAS), Beijing* 100029

[2] *Graduate University of Chinese Academy of Sciences, Beijing* 100049

(Received 30 April 2007; revised 17 September 2007)

ABSTRACT

The relationship between the North Asia cyclone (NAC) activity and the Southern Annular Mode (SAM) is documented in this research. The definition of the NAC index (NACI) is based on the atmospheric relative vorticity in North Asia. The analysis yields a significant positive correlation between previous winter Southern Annular Mode index (SAMI) and spring NACI in the interannual variability, with a correlation coefficient of 0.51 during 1948–2000. Analysis of the NAC-related and SAM-related atmospheric general circulation variability demonstrates such a relationship. The study further reveals that when the winter SAM becomes strong, the springtime atmospheric convection in tropical western Pacific will intensify and the local Hadley circulation will be strengthened. As a result, the abnormal subsiding motion over South China makes the temperature gradient intensified in the low level and strengthens the jet in the high level, both of which are beneficial to the development of NAC activity.

Key words: North Asia cyclone, Southern Annular Mode, atmospheric general circulation

DOI: 10.1007/s00376-008-0673-5

1. Introduction

The North Asia cyclone (NAC) is a very important synoptic phenomenon in Mongolia and North China. It is comparatively active in boreal spring (March–April–May), bringing gale-force winds, low temperatures, and occasional precipitation and severe dust storms over vast areas of China (Zhang, 1989; Liu et al., 2003; Wang and Guo, 2005). Case studies and diagnostic analyses revealed several synoptic factors favorable to the development of NAC, such as strong, low level fronts, cold vortex at high levels, warm air extending northward and so on (Zhang, 1984; Liu et al., 2003). Lin and Yang (1992) and Zhang (1984) did some statistical work about NAC, including source regions, frequency, lifetime, path and intensity. Recently, Wang and Guo (2005) and Yao et al. (2003) analyzed the climatic characteristics and variations of the frequency of extratropical cyclone over East Asia in spring and obtained some valuable conclusions. However, the climatic background and large scale physical processes related to NAC are still an open question and require further study.

The Southern Hemispheric (SH) annular mode (SAM), which is also called the Antarctic Atmosphere Oscillation (AAO), is more zonally symmetric and oscillates more strongly between middle and high latitudes than its counterpart in the Northern Hemisphere (NH) (Gong and Wang, 1999; Thompson and Wallace, 2000; Ambaum et al., 2001; Thompson and Solomon, 2002; Fan, 2007). SAM has been found to be linked with the climate not only in the SH but also in the NH. Xue et al. (2003a) indicated the significant correlations between the Mascarene (and Australian) High and rainfall in South China. Xue et al. (2003b) conducted a further study on such relationships by numerical simulation and found that the Mascarene subtropical high could exert influence on the subtropical high over the Western Pacific through low frequency propagation of the anomalies, which again affects the summer rainfall in the Yangtze River. SAM has also been found to be associated with the dust weather fre-

*Corresponding author: WANG Huijun, wanghj@mail.iap.ac.cn

quency as well as the surface air temperature and precipitation in central North China (Wang, 2001; Gao et al., 2003; Fan and Wang, 2004; Wang and Fan, 2005; Fan and Wang, 2006).

In this study, we focus on the cyclone activities in spring when NAC is most frequent and the monsoon and ENSO-related signals are weak as depicted by "spring predictability barrier" (Webster et al., 1998). Fan and Wang (2004) explored the relation between boreal winter-spring SAM and the dust weather in China, and found that the interannual variation of SAM played a significant role in the dust-related atmospheric circulation. Therefore, we are motivated by the question of whether there is linkage between SAM and NAC activity, which is closely related to the state of the atmospheric general circulation in NH and may bring more dust weather. The results will help us to understand the NAC-related climate variability.

2. Data and method

The primary dataset used in this study is the National Centers for Environmental Prediction/National Center for Atmospheric Research (NECP/NCAR) (Kalnay et al., 1996) reanalysis data at 17 vertical pressure levels and with a horizontal resolution of $2.5° \times 2.5°$. The temporal resolution for calculating NACI is 6 hours, which is shorter than the life time of an extratropical cyclone which is reasonable for the description of NAC. We also use monthly mean reanalysis data to analyze the NAC-related and SAM-related atmospheric circulation. Both kinds of data cover the period from January 1948 to December 2000. Bromwich and Fogt (2004) argue that there are strong trends in the skill of the NCEP/NCAR reanalysis in the high and middle latitudes of the SH from 1958 to 2001. To reduce such biases, we remove all the fields' linear trends so as to obtain the interannual variability.

The SAM is defined as the leading principal component (PC) of the monthly mean 850 hPa geopotential height anomaly field over the domain poleward of 20°S (Thompson and Wallace, 2000). In this research, the SAM index is obtained from http://www.jisao.washington.edu/aao/slp/aaoslppc1-9482002, whose length is also from January 1948 to December 2000. Marshall (2003) compares the SAM from observations with reanalyses and concludes that the SAM from reanalyses has both incorrect trend and seasonality. Based on such conclusions, the SAMI from Marshall (2003) is also used to demonstrate the robust relation between the SAM and the NAC activity.

The definitions of the cyclone activities have been well documented in the previous literatures (Zhang, 1984; Gulev et al., 2001; Yao et al., 2003; Löptien and Ruprecht, 2005; Wang and Guo, 2005). Most of these criterions are based on the variation of the sea level pressure (SLP). However, in this paper, a new index named as NAC index (NACI) is defined to describe the NAC activity. Different from previous definitions, this index is based on the relative vorticity of the atmosphere. As we know, when the NAC breaks out, the vorticity of the air at low level will become positive, which could be a good indication for the case.

Before going on, we need to find out the spatial domain of NAC. Zhang (1984) chose (30°–55°N, 80°–135°E) as the origin of NAC. Zhu et al. (1992) pointed out that most NACs break out and move around within (40°–55°N, 90°–135°E). Wang and Guo (2005) set (40°–55°N, 90°–140°E) as the main region for the NAC activities. Figure 1 is the climatological distribution of springtime 850 hPa vorticity in North Asia, which may roughly represent the spatial distribution of the cyclone activity. As the figure shows, there are two positive centers over the domain of (40°–55°N，90°–130°E), which are in good agreement with previous work as narrated above. As a result, we set (40°–55°N，90°–130°E) as the key region of NAC (KR), within which the area-weighted average vorticity is used to calculate the NACI. The main idea is that: when NAC happens, the vorticity of most grid points in the key area become positive making the sum significantly larger. The stronger the cyclone is, the longer the case will last. Based on this point, we define NACI as follows.

First, the area-weighted average vorticity in the KR are calculated from the 6-hourly NCEP/NCAR velocity at 850 hPa. We then make a 5-point running average over these results in every month, so as to remove the daily noise. For each month, we look through the time series to find out whether there are 4 or more continuous points which are positive and mark them all if yes (Because every NAC event lasts 1 day or more.). Finally, the number of all the marked points is summed up and divided by the length of the time series. After

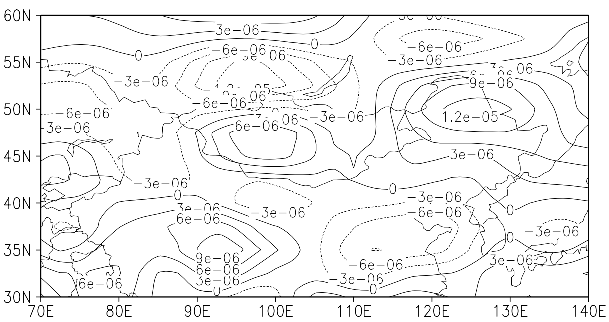

Fig. 1. Climatological distribution of 850 hPa vorticity in spring during 1948–2000. Units: s^{-1}.

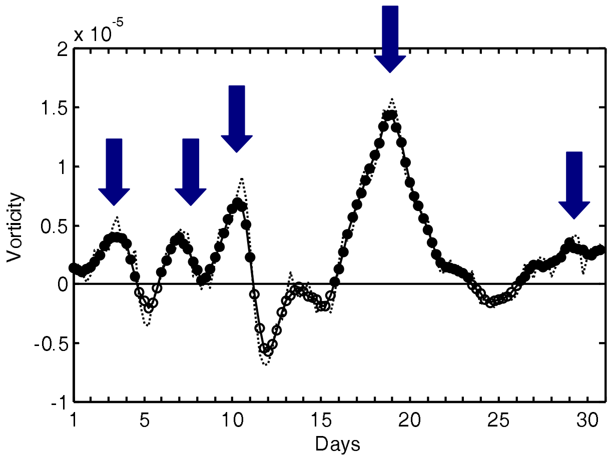

Fig. 2. The time series of the area-weighted average 850 hPa vorticity in the KR for April 1980. The dashed line indicates the exact values. The solid line is the 5-point running average. If there are at least 4 consecutive values above 0, then we use filled circles to mark them. Otherwise, we used the empty circles. Bold arrows indicate NAC events determined by traditional definition in that month.

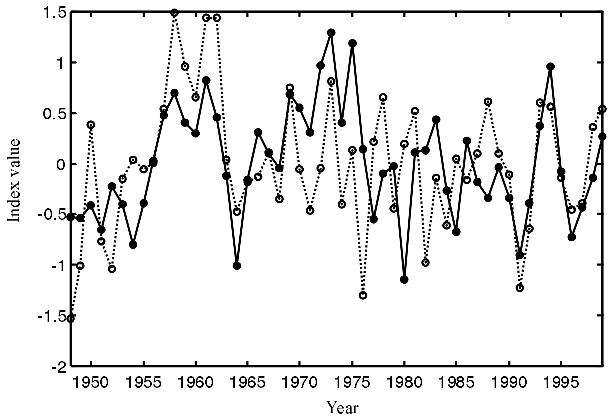

Fig. 3. Time series of winter SAMI (dotted line), and the following spring NACI (solid line). The years marked above correspond to the winter time, so "1950" means the winter of 1950/1951 for SAMI and the spring of 1951 for NACI.

normalization with respect to every calendar month is complete, the NACI is obtained.

This method is not complicated but has clear physical implications. Case studies show that NACI is suitable for the description of NAC activity, especially in spring. Figure 2 gives an illustration of the NACI of a specific month. As the figure shows, the temporal spans of the filled circles are in good agreement with the actual NAC events determined from the traditional definition (Zhang, 1984). In April 1980, there are a total of 5 NAC events, with a strong case during 16 April–21 April. So we calculate the percentage of the filled circles (that is 86/120) to obtain an indication for the intensity of the activity of the cold air in that month. We also use other physical variables such as SLP, geopotential height (HGT), temperature, divergence and so on to calculate the index. However, the variation of these variables in the KR could not correspond to the NAC events as well as that of vorticity. That's why we chose the latter to calculate NACI.

All the data, including NACI and the index of SAM (SAMI), are averaged for boreal winter months (December, January and February, or DJF) and spring months (March, April, and May, or MAM) respectively. Regression methods (See Thompson and Wallace, 2000 for detailed instruction of such methods) and composite analyses are conducted to analyze the NAC-related and SAM-related atmospheric general circulation variability. As for the latter, we select those non-ENSO years whose last winter SAMI is higher than 0.5 standard deviation (1958, 1959, 1960, 1961, 1962, 1974, 1979, 1989, 1994, 2000) or lower than −0.5 standard deviation (1952, 1966, 1977, 1980, 1985, 1992).

3. Results

Figure 3 shows the interannual variability of winter SAMI and the following spring NACI. The correlation coefficient for them is 0.51 at 99.9% significant level from a local student t-test. We calculated the power spectra of two indices. The spectra of both NACI-MAM and SAMI-DJF show peaks at approximately 3.5 years above 90% red noise confidence level, and the result of the latter has been reported by Gong and Wang (1999). The correlation between the observed SAMI of Marshall (2003) and the NACI is similar to the results shown above. The correlation coefficient is about 0.43 at 99.5% significant level from 1957 to 2000.

The leading modes of the singular value decomposition (SVD) analysis of the winter SLP anomaly field over the domain poleward of 20°S (denoted as left field) and the spring SLP anomaly field in North Asia (denoted as right field) are showed in Fig. 4. Both the homogeneous and the heterogeneous correlation patterns of the left field resemble the typical SAM pattern. The patterns of the right field indicate the fall of pressure over KR, which is one synoptic characteristic of the extratropical cyclone and usually used as a criterion for cyclone events (Zhang, 1984; Gulev et al., 2001; Yao et al., 2003; Löptien and Ruprecht, 2005). The first modes explain 78.92% of the covariance of two fields, as well as 34.77% and 27.61% of the vari-

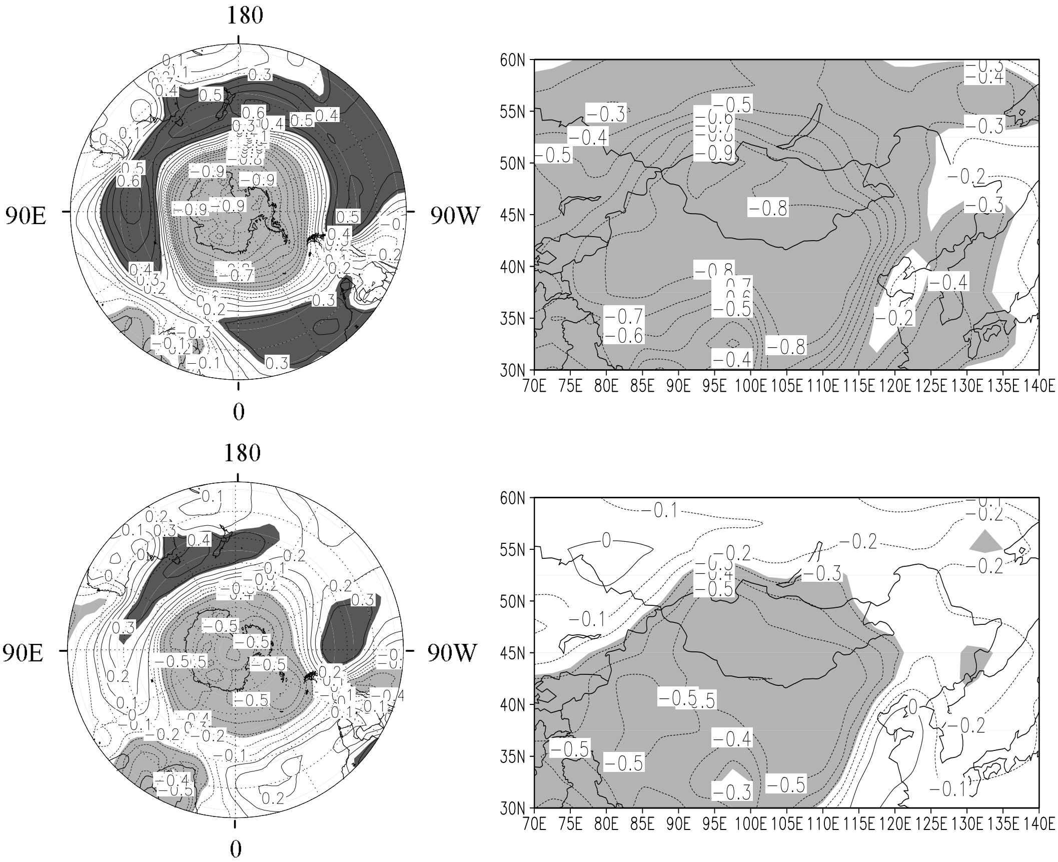

Fig. 4. (Top) Homogeneous correlation maps and (bottom) heterogeneous correlation maps of the leading SVD mode of the winter SH (poleward of 20°S) SLP anomalies and spring SLP anomalies over North Asia. Left panels are for the SH, right panels are for North Asia. Shading indicates correlation coefficients that pass the 95% significance level. Contour interval is 0.1 with negative contours dashed.

Table 1. The contribution from the first 5 SVD modes to the total squared covariance of the winter SH (poleward of 20°S) SLP anomalies (Left field) and spring SLP anomalies over North Asia (Right field) and to the variance of each.

SVD mode number	Contribution to total squared covariance (%)	Contribution to variance of left field (%)	Contribution to variance of right field (%)
1	78.92	34.77	27.61
2	7.09	6.76	12.37
3	5.15	5.43	19.11
4	2.62	5.77	10.24
5	2.09	5.16	6.64
Sum	95.87	57.89	75.97

ance of the left field and the right field respectively, as indicated in Table 1. The results show that the associated variability between these two fields takes up the main part of the individual variability of themselves. Hence, the SAM-related variability plays a major role in the variation of NAC activity.

Now we analyze the variation of the atmospheric circulation related to NAC and SAM. We first made analyses of the regressed HGT, temperature and wind velocity at different levels on NACI-MAM and SAMI-DJF respectively. Figure 5 shows the regressed fields at 850 hPa onto the variation of SAM in boreal winter. When the SAM becomes stronger than normal, there will be a vast drop of HGT over the KR, which is similar to the SLP pattern of the SVD analyses shown in Fig. 4. Meanwhile, the temperature becomes lower and higher than normal in the north and south part of the KR respectively, increasing the meridional gra-

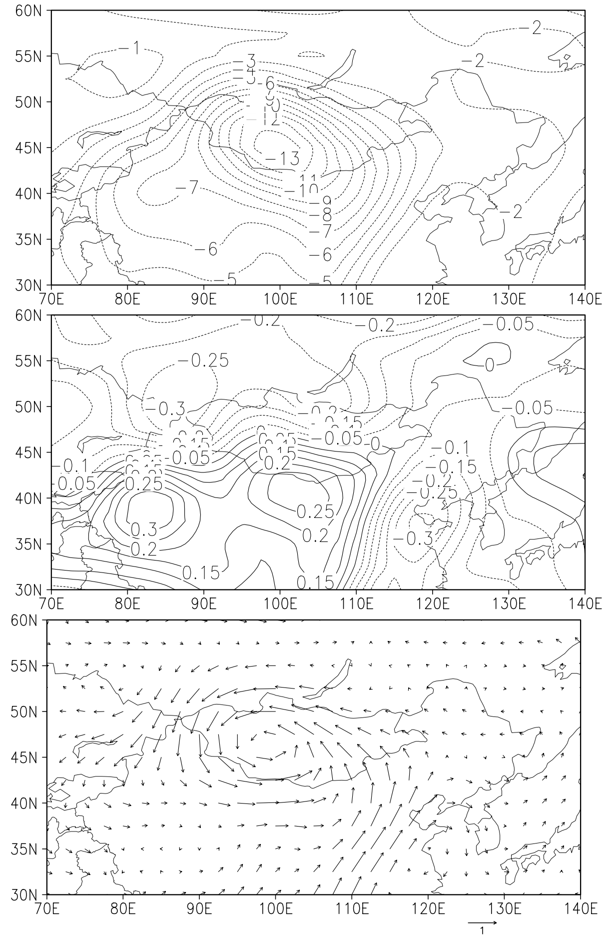

Fig. 5. Regression maps for spring 850 hPa geopotential height (top), temperature (middle) and wind velocity (bottom) onto the normalized winter SAMI during 1948–1999. Negative contours are dashed.

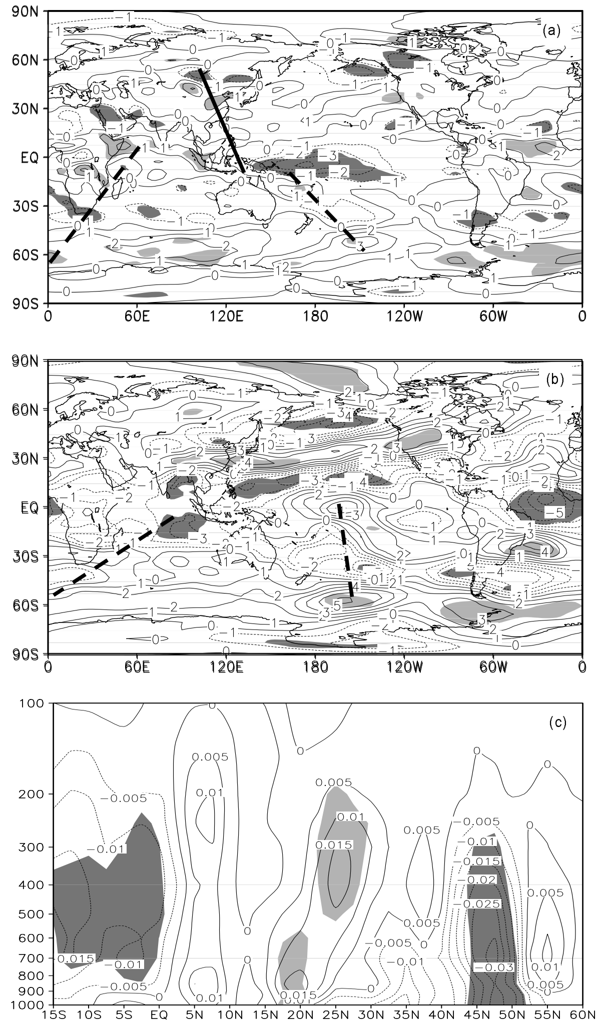

Fig. 6. (a) Composite difference of spring 850 hPa zonal wind by winter SAMI (m s^{-1}). (b) The same as (a) but for the 200 hPa wind composite. (c) Composite difference of spring ω (Pa s^{-1}) within the slice denoted by the thick solid line in (a). Shadings indicate 95% significant level. Negative contours are dashed.

dients and intensifying the baroclinicity of the air in the KR, and thus is favorable to the development of NAC. As a result, the cyclonic circulation is established as shown in the wind velocity regression map. The regression map onto the NACI-MAM shows a clearly SAM-like pattern over the high latitudes of SH (figures not shown), which again demonstrates the relationship between SAM and NAC activity.

In the following part of this section, we will discuss the composite differences of the circulation fields upon the winter SAMI. As mentioned before, we excluded the ENSO years in order to rule out the possible impact of ENSO cycle. Figure 6a shows the springtime 850 hPa composite zonal wind difference between the high and low winter SAMI. We can find the abnormal wind convergence at the region north of Australia. However, the composite analysis of 200 hPa zonal wind shows the anomalous divergence at the same region (see Fig. 6b). Such wind structure suggests reinforced convection taking place in the tropical western Pacific (TWP), which may change the East Asia circulation through the Pacific-Japan (PJ) wave pattern (Nitta, 1987; Huang and Sun, 1994). We drew a thick solid line through the KR and TWP to get a vertical slice. The SAMI-based composite of vertical velocity ω within the slice is showed in Fig. 6c. There are abnormal rising motions in TWP (15°–0°S) and subsidence in the subtropical region of NH (15°–30°N), which indicates a strengthened local Hadley circulation. As a result, the intensified downdraft will increase the HGT of air and warm the atmosphere in the South China, both of which help to increase the intensity of the front at low levels and excite more NACs. Besides, the downdraft could strengthen the subtropical upper-level front and accelerate the East Asia upper-level jet as a result, which could be seen from the 200 hPa zonal wind composite map as showed in Figure 6b. The accelerated upper jet stream is helpful for the frontogenesis in the low level (Zeng, 1979; Gao and Tao, 1991).

On the other hand, we need to know the connection between TWP and SAM. Taking a second look at Fig. 6a, we can see two wave trains bridging over the circumpolar westerlies at high latitudes of SH and the wind anomalies in the tropical regions (see the thick dashed lines in figure). One is over the south Pacific and the other is over the west India Ocean, the former of which was indicated by Wang and Fan (2005). Both wave trains could also be seen in the high levels as well, though the strength is a little weaker than the ones in 850 hPa (see Fig. 6b).

4. Conclusion

In this paper, we defined a new index to describe the North Asia cyclone activities and explored the relationship between springtime NAC and SAM. The result reveals a significant positive correlation between the interannual variability of NAC activity and SAM. To testify to such a relationship, the variation of related atmospheric circulation was analyzed. Analyses of physical variables including SLP, HGT, temperature and the wind velocity all support the correlation analysis.

It is suggested that there is abnormal convection in the TWP when SAM becomes strong in the previous winter, and the anomalous convection strengthens the local Hadley circulation and helps to increase the baroclinicity of air to promote frontogenesis in the low levels of North Asia. The reinforced meridional circulation also intensifies the upper-level jet stream, which is favorable to the development of NAC at low levels.

Acknowledgements. This research was jointly supported by the National Natural Science Foundation of China under Grant Nos. 40631005 and 40620130113, and CAS International Partnership Project.

REFERENCES

Ambaum, M. H. P., B. J. Hoskins, and D. B. Stephenson, 2001: Arctic Oscillation or North Atlantic Oscillation? *J. Climate*, **14**, 3495–3507.

Bromwich, D. H., and R. L. Fogt, 2004: Strong trends in the skill of the ERA-40 and NCEP-NCAR reanalyses in the high and middle latitudes of the Southern Hemisphere, 1958–2001. *J. Climate*, **17**, 4603–4619.

Fan, K., and H. J. Wang, 2004: Antarctic oscillation and the dust weather frequency in North China. *Geophys. Res. Lett.*, **31**, L10201, doi:10.1029/2004GL019465.

Fan, K. and H. J. Wang, 2006: Interannual variability of Antarctic Oscillation and its influence on East Asian climate during boreal winter and spring. *Science in China* (D), **49**(5), 554–560, DOI: 10.1007/s11430-006-0554-7.

Fan, K., 2007: Zonal asymmetry of the Antarctic Oscillation. *Geophys. Res. Lett.*, **34**, L02706, doi:10.1029/2006GL028045.

Gao, H., F. Xue, and H. J. Wang, 2003: Influence of interannual variability of Antarctic oscillation on mei-yu along the Yangtze and Huaihe River valley and its importance to prediction. *Chinese Science Bulletin*, **31**, 61–67.

Gao, S. T., and S. Y. Tao, 1991: The lower layer frontogenesis induced by the acceleration of upper jet stream. *Chinese J. Atmos. Sci.*, **15**(2), 11–22. (in Chinese)

Gong, D. Y., and S. W. Wang, 1999: Definition of Antarctic Oscillation index. *Geophys. Res. Lett.*, **26**, 459–462.

Gulev, S. K., O. Zolina, and S. Grigoriev, 2001: Extratropical cyclone variability in the Northern Hemisphere winter from the NCEP/NCAR reanalysis data. *Climate Dyn.*, **17**, 795–809.

Huang, R. H., and F. Y. Sun, 1994: Impacts of the thermal state and the convective activities in the tropical western warm pool on the summer climate anomalies in East Asia. *Chinese J. Atmos. Sci.*, **18**(2), 141–151. (in Chinese)

Kalnay, E., and Coauthors, 1996: The NCEP/NCAR 40-year reanalysis project. *Bull. Amer. Meteor. Soc.*, **77**, 437–471.

Lin, M. Z., and K. M. Yang, 1992: Synoptic and climatic analysis of the North China cyclone. *Meteorology*, **18**(5), 20–26. (in Chinese)

Liu, J. T., X. J. Zhen, L. Kang, X. G. Jiang, F. Y. Qi, and X. Fang, 2003: A case study of a severe dust storm resulted from an explosive Mongolia Cyclone. *Climatic and Environmental Research*, **8**(2), 218–229. (in Chinese)

Löptien, U., and E. Ruprecht, 2005: Effect of synoptic systems on the variability of the North Atlantic Oscillation. *Mon. Wea. Rev.*, **133**(10), 2894–2904.

Marshall, G. J., 2003: Trends in the southern annular mode from observations and reanalyses. *J. Climate*, **16**, 4134–4143.

Nitta, T., 1987: Convective activities in tropical western Pacific and their impact on the Northern Hemisphere summer circulation. *J. Meteor. Soc. Japan*, **65**, 373–390.

Thompson, D. W. J., and J. M. Wallace, 2000: Annular modes in the extratropical circulation: Part I: month-to-month variability. *J. Climate*, **13**, 1000–1016.

Thompson, D. W. J., and S. Solomon, 2002: Interpretation of recent Southern Hemisphere climate change. *Science*, **296**, 895–899.

Wang, H. J., 2001: The weakening of Asian monsoon circulation after the end of 1970s. *Adv. Atmos. Sci.*,

18(3), 374–386.

Wang, H. J., and K. Fan, 2005: Central-north China precipitation as reconstructed from the Qing dynasty: Signal of the Antarctic Atmospheric Oscillation. *Geophys. Res. Lett.*, **32**, L24705, doi:10.1029/2005GL024562.

Wang, Y. L., and P. W. Guo, 2005: Climatic characteristics of northern cyclone activity in Spring and their relationship to rainfall and temperature in China. *Journal of Nanjing Institute of Meteorology*, **28**(3), 391–397. (in Chinese)

Webster, P. J., V. O. Magana, T. N. Palmer, J. Shukla, R. A. Tomas, M. Yanai, and T. Yasunari, 1998: Monsoons: Processes, predictability, and the prospects for prediction. *J. Geophys. Res.*, **103**, 14451–14510.

Xue, F., H. J. Wang, and J. H. He, 2003a: Interannual variability of Mascarene High and Australian High and their influence on the East Asian summer rainfall over East Asia. *Chinese Science Bulletin*, **48**(5), 492–497.

Xue, F., D. B. Jiang, X. M. Lang, and H. J. Wang, 2003b: Influence of Mascarene high and Australian high on the summer monsoon in East Asia: Ensemble simulation. *Adv. Atmos. Sci.*, **20**(5), 799–809.

Yao, S. X., Y. C. Zhang, and T. J. Zhou, 2003: Climatic characteristic of Extratropical cyclone frequency and its variations over East Asia during recent 50 years in spring. *Journal of Nanjing Institute of Meteorology*, **26**(3), 317–323. (in Chinese)

Zeng, Q. C., 1979: *Physical and Mathematical Basis of Numerical Weather Prediction*. Science Press, Beijing, 543pp. (in Chinese)

Zhang, S. Y., 1984: Several statistical feature of the North China cyclone and the synoptic analysis of its development. *Plateau Meteorology*, **3**(3), 83–89. (in Chinese)

Zhang, S. Y., 1989: Relationship between the springtime North China cyclone activity and the precipitation. *Chinese. J. Atmos. Sci.*, **13**(2), 247–251. (in Chinese)

Zhu, Q. G., J. R. Lin, S. W. Shou, and D. S. Tang, 1992: *Principles and Methodology of Synoptic Meteorology*. China Meteorologicae Press, Beijing, 534pp. (in Chinese)